Properties of Carbon Nanofibers Prepared from Electrospun Polyimide

G. S. Chung,[1] S. M. Jo,[2] B. C. Kim[1]

[1]*Division of Applied Chemical Engineering, Hanyang University, 17 Haingdang-dong, Seongdong-gu, Seoul 133-791, Korea*
[2]*Polymer Hybrid Center, Korea Institute Science and Technology, Seoul 136-791, Korea*

Received 18 September 2003; accepted 20 June 2004
DOI 10.1002/app.21742
Published online in Wiley InterScience (www.interscience.wiley.com).

ABSTRACT: A solution of a polyimide (PI, Matrimid® 5218) in dimethylacetamide was electrospun, and carbonization of the electrospun nonwoven fabrics produced carbon nanofiber fabrics. The effects of iron(III) acetylacetonate (AAI) on carbonization and the resulting morphology were also investigated. The carbonization behavior of the nonwoven fabrics was examined by X-ray diffraction and Raman spectroscopy. AAI promoted carbonization of the nonwoven fabrics and increased the carbon yield. Addition of 3 wt % AAI increased the crystal dimension of electrospun PI nanofibers from 1.06 to 4.18 nm and decreased the integrated intensity ratio from 3.37 to 1.83 when heat treated at 1200°C. Scanning electron microscopy images of the carbonized nonwoven fabrics showed that AAI remained as particles within the fibers after carbonization. In addition, transmission electron microscopy observations revealed that turbostratic-oriented graphite layers were observed around the particles even at 1200°C, which have been reported only on carbonization of rigid-chain solvent insoluble PI materials under tension. © 2005 Wiley Periodicals, Inc. J Appl Polym Sci 97: 165–170, 2005

Key words: solvent soluble polyimide; electrospinning; carbon nanofiber fabric; turbostratic-oriented graphite structure; iron catalyst

INTRODUCTION

Carbon fibers have been used in a variety of fields' as high-performance and functional materials. Woven or nonwoven carbon fibers are used as absorbed materials because of better adsorption capacity than conventional activated granular and powder carbon materials. They are being applied to gas separation and liquid adsorption. Because thinner fibers are more desirable for those separation and adsorption applications, there has been growing interest in electrospinning to produce ultrafine fibers.[1,2] The electrospun nonwoven polyimide (PI) fabrics composed of nanofibers may be carbonized by a single step because of the extreme thinness of individual fibers. Thus, such electrospun polymeric nanofibers may be used as effective precursors of carbon nanofibers.

PI is a good candidate for a carbon precursor. However, most of the solvent insoluble PIs such as Kapton® are insoluble in organic solvents, which is a prerequisite for electrospinning. A thermotropic PI (Matrimid® 5218) can be dissolved in an organic solvent such as dimethylacetamide (DMAc), and the PI solution can be readily electrospun to produce nanofibers. In addition, a transition metal would promote carbonization and graphitization of PI, which was verified for Kapton® films by various research groups.[3–7] However, there has been no attempt to produce carbon nanofiber fabrics by electrospinning of solvent soluble PIs and subsequent carbonization. This study investigates structural changes of electrospun nonwoven PI fabrics with the heat treatment temperature (HTT) and the effects of a transition metal, Iron(III) acetylacetonate (AAI) on the carbonization behavior of the fabrics.

EXPERIMENTAL

Preparation of electrospun nonwoven fabrics

A solvent soluble PI (Matrimid® 5218) powder (Ciba Specialty Co.) was the precursor material for carbonization, whose chemical structure is given below:

Correspondence to: B. C. Kim (bckim@hanyang.ac.kr).

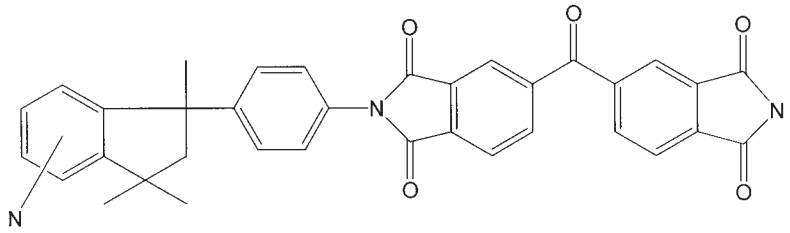

The solvent soluble PI was dissolved in DMAc, and AAI ($[CH_3COCH{=}C(O{-})CH_3]_3Fe$) was mixed into the solution. The polymer concentration was 20 wt % and the catalyst levels were 0.3, 0.6, 1.0, 1.5, 2.0, and 3.0 wt % on the weight of the polymer. The PI solution was first placed in a 25-mL syringe with a 20-gauge needle. A Betran series 205B high voltage power supply was used to produce voltage ranging from 6.0 to 15.0 kV. The PI solution was suspended under constant pressure onto the electrically ground collector at 24°C below a relative humidity of 24%. The flow rate was 20–50 μm/min. Electrospun nonwoven fabrics were dried under a vacuum at 60°C for 12 h to produce 60 μm thick fibers. The fabrics were coded as PI-FE-*X*-*Y*, in which *X* denotes the weight percent of AAI and *Y* denotes the HTT.

Electrospun nonwoven PI fabrics were carbonized over the temperature range of 400–1200°C in a high-purity argon atmosphere. The heating rate was 2°C/min, and the samples were held at each HTT for 1 h.

Characterization of electrospun nonwoven fabrics

The thermal decomposition behavior of electrospun nonwoven PI fabrics up to 1300°C was analyzed by dynamic thermal analysis and thermogravimetric analysis (TGA, TA Instrument) at a heating rate of 10°C/min in a nitrogen atmosphere. The carbon yield was determined by reduction of the weight of the fabrics after carbonization.

The change of the structure of the electrospun nonwoven PI fabrics with temperature was examined by X-ray diffraction (XRD) diffractometer and Raman spectroscope. The XRD patterns were determined with an Mx-018 X-ray diffractometer (MACscience) with CuKα radiation (λ = 0.15406 nm, 40 kV, 200 mA) over the 2θ range of 10–90°. Raman spectra were obtained by micro-Raman (Jbon–Yvon Spex T64000) using an argon laser as an illumination source, which consisted of a subtractive dispersion triple monochromator combined with a spectrograph that disperses the light onto a bidimensional CCD detector cooled at 140 K. The laser frequency was the 514.532-nm line, and the laser spot diameter reaching the sample was about 3.5 μm.

The fiber surface was observed by a field-emission scanning electron microscopy (FE-SEM) microscope (Hitachi S-4200). SEM images of the specimens heat treated at 1200°C were taken in the longitudinal and rupture cross-sectional directions.

RESULTS AND DISCUSSION

Thermal properties of electrospun PI nonwoven fabric

Figure 1 illustrates the TGA curves of PI-Fe-0 and PI-Fe-3. In the case of the PI-Fe-0, weight loss mostly takes place in the temperature range of 450–720°C because of imide ring cleavage, which accords with previous reports.[8] The evolution of CO and C—N bonds causes imide ring cleavage. Of the two specimens, PI-Fe-3 exhibits greater weight loss below 200°C than PI-Fe-0. This is ascribed to the decomposition of the acetylacetonate contained in AAI. However, it is interesting to see that PI-Fe-3 gives a higher ultimate carbon yield than PI-Fe-0 above 1200°C, indicating that AAI is an effective catalyst of carbonization for solvent soluble Matrimid®, as well as solvent insoluble Kapton®.[3] Actual carbonization of the sample in the bench-scale furnace also gives the same result.

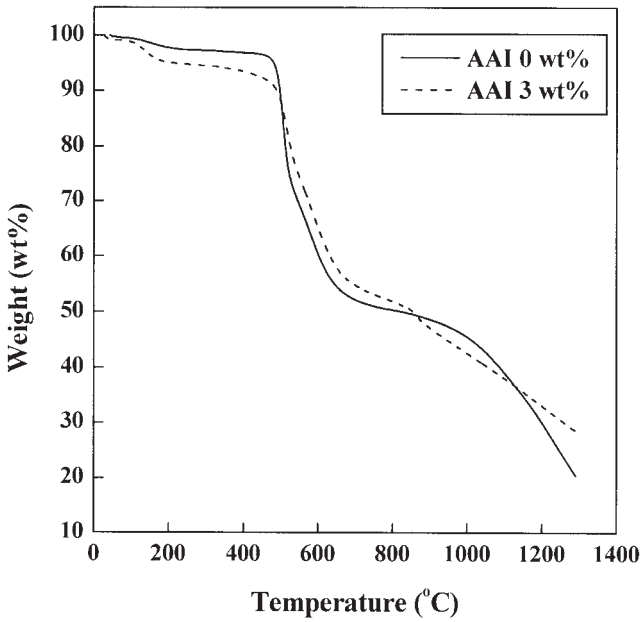

Figure 1 The variation of the weight of electrospun nonwoven PI-Fe-0 and PI-Fe-3 fabrics with the temperature.

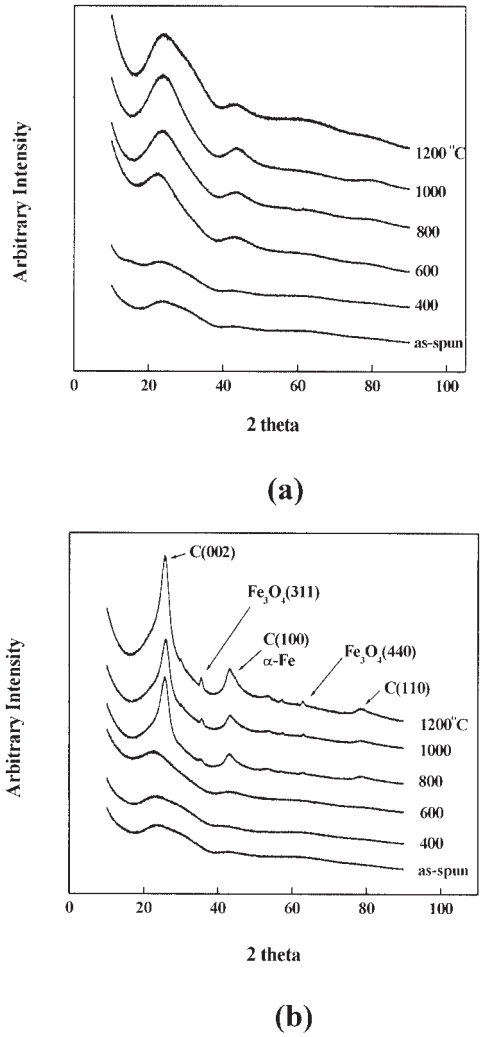

Figure 2 XRD patterns of electrospun fabrics with the temperature for (a) PI-Fe-0 and (b) PI-Fe- 3.

TABLE I
Variation of Average Interlayer Spacing d_{002} and Average Crystallite Size along *c*-Axis (L_c) with Temperature for Carbon Nonwoven Fabrics Prepared from Electrospun PI-Fe-0 and PI-Fe-3

		Carbon 002[a]				Carbon 002	
HTT (°C)	AAI (wt %)	d_{002} (nm)	L_c (nm)	HTT (°C)	AAI (wt %)	d_{002} (nm)	L_c (nm)
800	0	0.37	1.04	1200	0.3	0.34	1.21
1000	0	0.37	1.09	1200	0.6	0.34	2.16
1200	0	0.37	1.06	1200	1.0	0.34	3.78
800	3	0.34	3.56	1200	1.5	0.34	4.14
1000	3	0.34	3.74	1200	2	0.34	4.07
1200	3	0.34	4.18	1200	3	0.34	4.18

[a] Carbon 002 is the 002 diffraction plane.

Microstructure of carbon fiber in nonwoven fabric

Figure 2(a, b) shows XRD patterns of electrospun PI fibers (PI-Fe-0, and PI-Fe- 3) with HTT, respectively. The XRD patterns of as-spun PI-Fe-0 in Figure 2(a) exhibit an amorphous halo in the 2θ range of 15° and 30°. This indicates that few structural changes take place up to 400°C in the absence of AAI. In the profiles of PI-Fe-0-600, 800, 1000, and 1200, however, the intensity of the peak in the vicinity of 23° increases with increasing temperature, indicating that carbonization takes place above 600°C. It is recognized that PI-Fe-0 develops only a noncrystalline structure composed of minute basic structural units under 1200°C.[9–11]

Up to 600°C, PI-Fe-3 gives XRD patterns similar to PI-Fe-0, as shown in Figure 2(b). At 800°C, however, a sharp peak by the 002 diffraction plane of carbon appears. In addition, the intensity of the peak increases with the HTT, although the shape is still asymmetric. Above 800°C, the peaks assigned to iron components such as α-Fe (metallic iron) and Fe_3O_4 are more noticeable. XRD peaks for Fe_3O_4 in the case of PI-Fe-3 above 800°C are related to residual oxygen in the furnace.[12]

Estimates of the mean crystallite dimensions (L_c) were obtained from powder XRD data by the Debye–Scherrer equation.[13] The values of d_{002} and L_c determined from the 002 peak after corrections are given in Table I. In the absence of AAI, d_{002} and L_c remain almost constant up to 1200°C (0.37 and 1.04–1.06 nm, respectively). The temperature independence of L_c suggests that the PI fabrics without an iron complex generate only noncrystalline structures. Addition of AAI decreases the d_{002} indicating the fiber structure gets denser. In addition, the L_c increases from 1.04 to 4.18 nm when increasing the AAI content from 0 to 3 wt %, indicating that the transition metal catalyzes

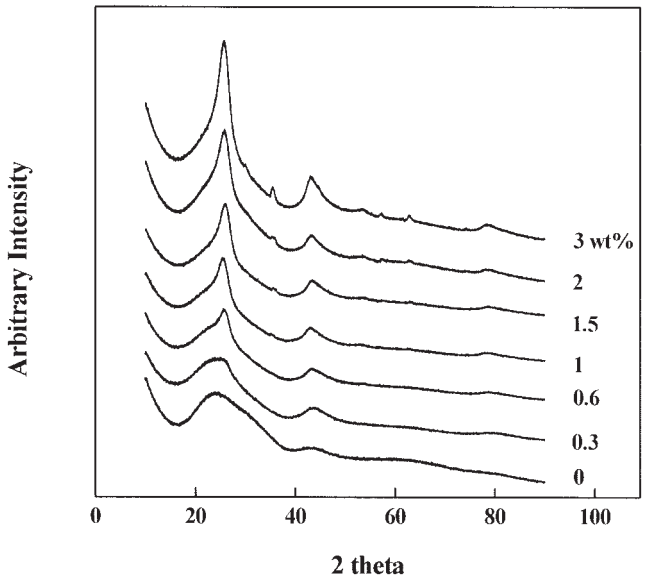

Figure 3 XRD patterns of electrospun fabrics with the AAI content at 1200°C.

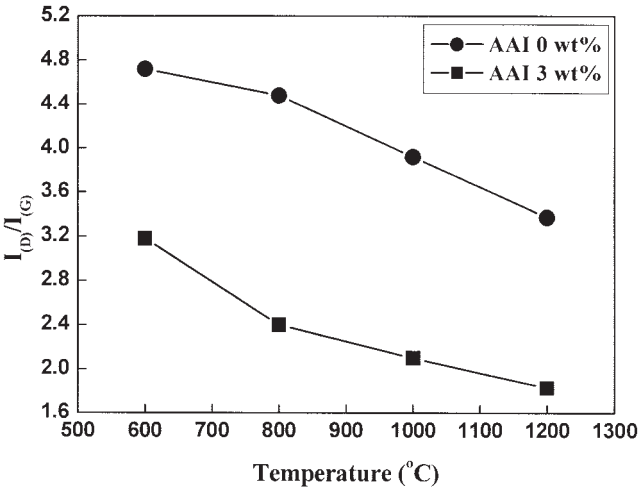

Figure 4 The variation of $I_{(D)}/I_{(G)}$ of PI-Fe-0 and PI-Fe-3 with the temperature.

carbonization of PI. In the case of PI-Fe-3, the value of d_{002} remains constant (0.34 nm) but L_c increases from 3.56 to 4.18 nm when the HTT increases from 800 to 1200°C. The XRD patterns in Figure 3 further ascertain the catalytic activity of the transition metal. As the AAI content is increased the intensity of the peak for carbon is increased and gets sharper. The values of d_{002} and L_c indicate that the carbonized nonwoven fabric includes a turbostratic structure that has a 2-dimensional orientation order.

The crystalline structure of graphite is well characterized by Raman spectroscopy.[14] The first-order band (E_{2g2}) of single hexagonal crystal graphite in the Raman active appears at 1582 cm^{-1} and weak bands appear at 42 (E_{2g}) and 2724 cm^{-1}.[15–19] The mode at 1582 cm^{-1} is called the *G* mode. A band around 1357 cm^{-1} is called the *D* mode by disorder-induced scattering, which is due to imperfection or lack of hexagonal symmetry in the carbon structure, resulting in breaking the *k*-momentum conservation. A wide Gaussian band (*M* mode) is considered as an amorphous carbon contribution.[14] The integrated intensity ratio ($I_{(D)}/I_{(G)}$) is one of the most important parameters characterizing not only the extent of order of the carbon structure but also defects in the material.

Figure 4 plots the $I_{(D)}/I_{(G)}$ of electrospun PI fibers against HTT. In the case of PI-Fe-0, increasing the HTT slightly decreases the $I_{(D)}/I_{(G)}$. However, the $I_{(D)}/I_{(G)}$ of PI-Fe-3 is notably decreased (from 3.18 to 1.83 nm) as the HTT is increased from 600 to 1200°C. It is also noted in Figure 5 that increasing the AA1 content increases the crystal size along the *a*-axis. These two figures quantitatively prove that AAI promotes carbonization of PI.

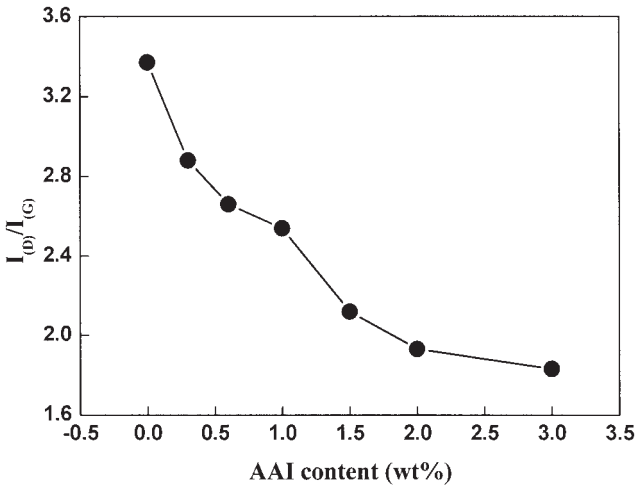

Figure 5 The variation of $I_{(D)}/I_{(G)}$ of electrospun PI fabrics with AAI content at 1200°C.

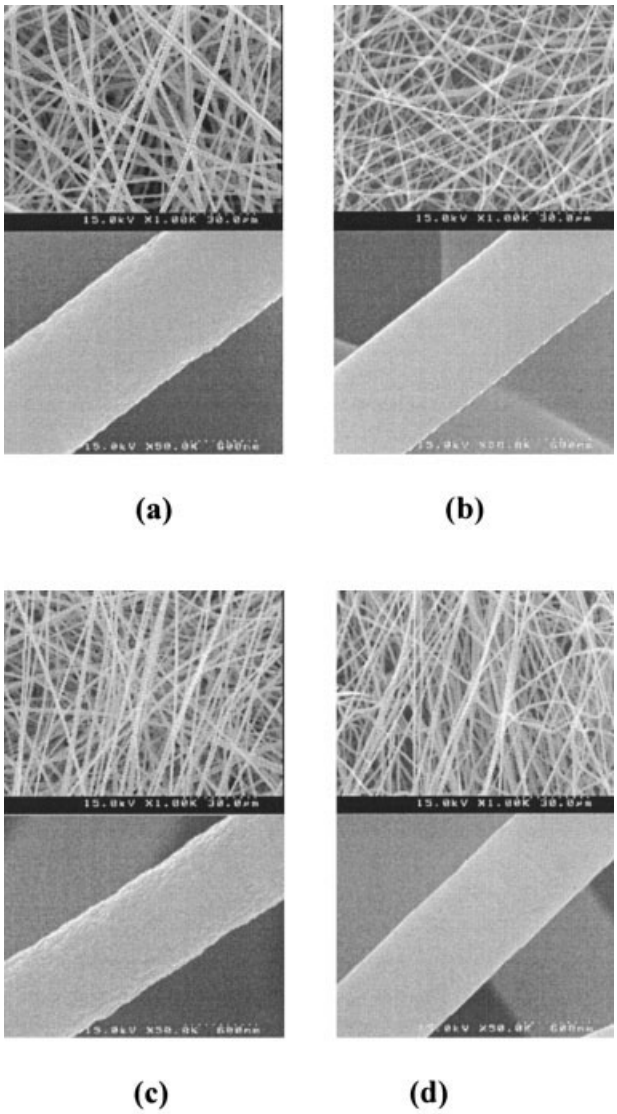

Figure 6 SEM micrographs of electrospun fabrics (a) PI-Fe-25, (b) PI-Fe-0-1200, (c) PI- Fe-3-25, and (d) PI-Fe-3-1200.

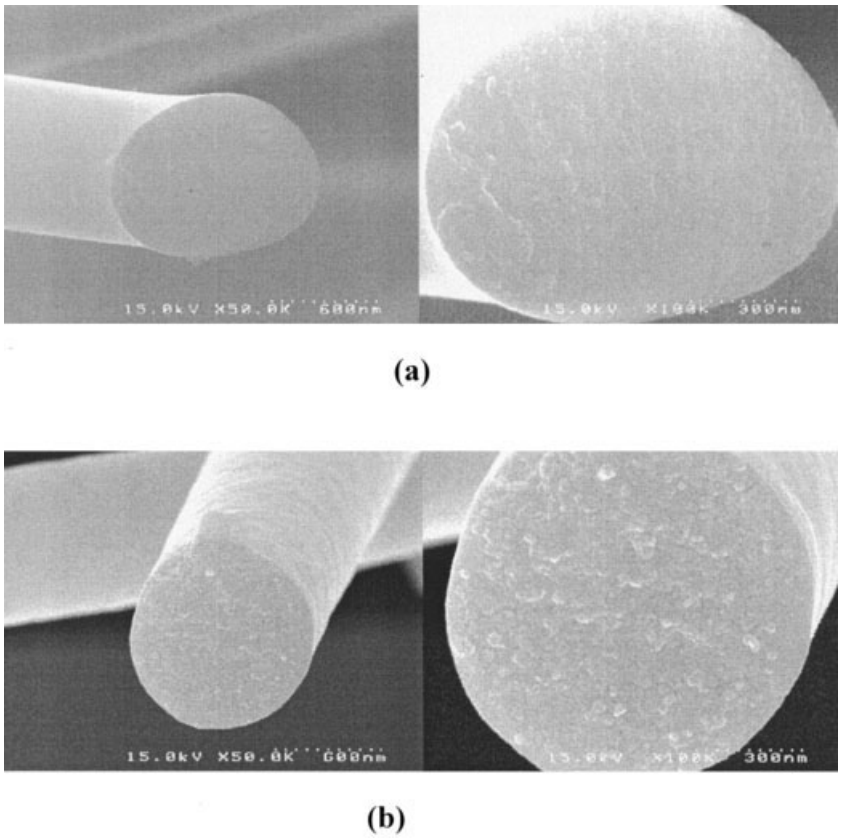

Figure 7 SEM micrographs of the cross-sectional surface of electrospun fabrics (a) PI-Fe-0-1200 and (b) PI-Fe-3-1200.

Morphology of carbon nonwoven fabric

Figure 6 shows SEM micrographs of electrospun PI-Fe-0 nonwoven fabric and fiber. Heat treatment makes the fiber surface smooth and slightly decreases the fiber thickness. This suggests densification of the fibers. PI-Fe-3 gives a similar result. It is worth mentioning in figure 6(b) that adherence of fibers takes place when heat treated at 1200°C in the absence of

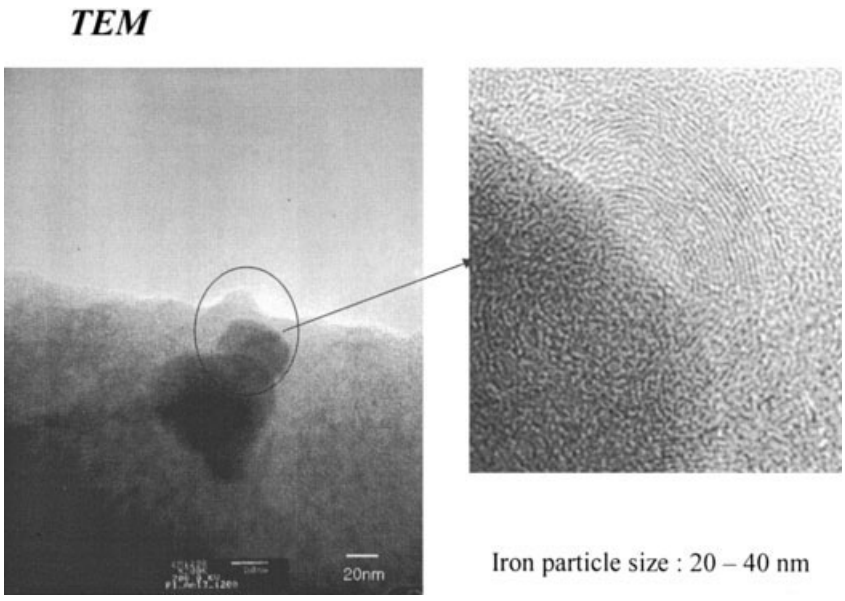

Figure 8 TEM images of electrospun PI-Fe-3-1200 fabrics.

AAI. By contrast, PI-Fe-3 gives less adherence of fibers as shown in figure 6(d). Figure 7 shows rupture cross sections of electrospun PI-Fe-0 and PI-Fe- 3 fibers heat treated at 1200°C. PI-Fe-3 produces more a noticeable grainy structure than PI-Fe-0. The size of the grains is about 30 nm.

Figure 8 shows TEM images of PI-Fe-3 heat treated at 1200°C. Clusters of AAI particles are observed, and the average size of the AAI particles is about 30 nm. This confirms that the grains observed in Figure 7(b) are AAI particles. The outer region of PI-Fe-3 fibers consists of a graphite-like concentration, which forms a turbostratic-oriented graphite layer even though the fabric is made of a flexible solvent soluble PI. This structure has been reported only on carbonization of rigid solvent insoluble PIs such as Kapton®.[9] That is, the solvent insoluble PI is a rigid-chain polymer, so it readily produces an ordered structure when heat treated under tension. However, solvent soluble PIs such as Matrimid® are known not to produce such ordered structures by carbonization because of chain flexibility. However, this result indicates that the electrospun thermoplastic PI nanofibers containing AAI can form an ordered structure during carbonization. The reason for developing the turbostratic structure seems to be related to the characteristic features of electrospun fabrics. That is, extreme thinness and porosity of the fabrics together with catalytic action of AAI lead to effective carbonization. In contrast, the regions close to the iron particles are composed of the disordered carbon layers, suggesting that AAI particles interfere with the perfectly ordered carbon layer.

CONCLUSION

Electrospinning and subsequent carbonization of PI solutions in DMAc offered a good way to procure carbon fabrics made of nanofibers. AAI proved to be a good promoter of carbonization of the electrospun PI fabrics. A careful examination of the resulting carbon structure by TEM suggested that a turbostratic structure was developed, which was observed only when solvent insoluble PIs were carbonized under tension. This seems to result from the extreme thinness of the electrospun fibers and effective carbonization by the presence of porosity in the electrospun fabrics. This result would contribute to the development of fabrics composed of carbon nanofibers.

References

1. Simm, W.; Gösling, C.; Bonart, R.; Falkai, B. U.S. Pat. 4,069,026, 1978.
2. Gibson, P. W.; Schreuder-Gibson, H.; Rivin, D. Colloid Surface A 1999, 187–188, 469.
3. Oka, H.; Inagaki, M.; Kaburagi, Y.; Hishiyama, Y. Solid State Ionics 1999, 121, 157.
4. Kaburagi, Y.; Hishiyama, Y.; Oka, H.; Inagaki, M. Carbon 2001, 39, 593.
5. Konno, H.; Shiba, K.; Kaburagi, Y.; Hishiyama, Y.; Inagaki, M. Carbon 2001, 39, 1731.
6. Yang, K. S.; Edie, D. D.; Lim, D. Y.; Kim, Y. M.; Choi, Y. O. Carbon 2003, 41, 2039.
7. Reshetenko, T. V.; Avdeeva, L. B.; Ismagilov, Z. R.; Pushkarev, V. V.; Cherepanova, S. V.; Chuvilin, A. L.; Likholobov, V. A. Carbon 2003, 41, 1605.
8. Hatori, H.; Yamada, Y.; Shiraishi, M.; Yoshihara, M.; Kimura, T. Carbon 1996, 34, 201.
9. Hishiyama, Y.; Igarashi, K.; Kaneko, I.; Fujii, T.; Kaneda, T.; Koidezawa, T.; Shimazawa, Y.; Yoshida, A. Carbon 1997, 35, 657.
10. Yoshida, A.; Kaburagi, Y.; Hishiyama, Y. Carbon 1991, 29, 1107.
11. Bourgerette, C.; Oberlin, A.; Inagaki, M. J Mater Res 1992, 7, 1158.
12. Kaburagi, M.; Hatori, H.; Yoshida, A.; Hishiyama, Y.; Inagaki, M. Synth Met 2001, 125, 171.
13. Oberlin, A.; Bonnamy, S.; Lafdi, K. In Carbon Fibers, 3rd ed.; Donnet, J. B.; Wang, T. K.; Rebouillat, S.; Peng, J. C. M. Ed.; New York: Marcel Dekker, 1998; Chapter 2.
14. Jawhari, T.; Roid, A.; Casado, J. Carbon 1995, 33, 1561.
15. Tuinstra, F.; Koening, J. L. 1970, 53, 1126.
16. Diollon, R. O.; Woollam, J. A. Phys Rev B 1984, 29, 3482.
17. Nistor, L. C.; Landuyt, J. V.; Ralchenko, V. G.; Kononenko, T. V.; Obraztsova, E. D.; Strelnitsky, V. E. Appl Phys A 1994, 58, 137.
18. Tzeng, S. S.; Pan, J. H. Mater Chem Phys 2002, 74, 214.
19. Hirose, T.; Fujino, T.; Fan, T.; Endo, H.; Okabe, T.; Yoshimura, M. Carbon 2002, 40, 761.